Presented at the "XIVth Rencontre de Moriond" March 11-23, 1979

ISTITUTO NAZIONALE DI FISICA NUCLEARE
Laboratori Nazionali di Frascati

LNF-79/25(P)
30 Aprile 1979

M. Spinetti: RESULTS FROM ADONE. -

Servizio Documentazione
dei Laboratori Nazionali di Frascati

INFN - Laboratori Nazionali di Frascati
Servizio Documentazione

LNF-79/25(P)
30 Aprile 1979

M. Spinetti: RESULTS FROM ADONE. -

Presented at the "XIVth Rencontre de Moriond" (March 11-23, 1979).

ABSTRACT.

A review of results from Adone is given. Topics covered are:

a) limits on $e^* \rightarrow e\gamma$;

b) R values;

c) multiplicities and G parities;

d) partial cross sections.

1. - INTRODUCTION.

This talk is a report on the following topics, concerning the Adone e^+e^- storage ring[1]:

a) new limits on $e^* \rightarrow e\gamma$;

b) R values;

c) multiplicities, G-parities;

d) partial cross sections.

Data taking is stopped since June 1978. At 1.5 GeV the machine has an average luminosity of $\sim 1\ nb^{-1}/day$, an energy spread of 0.8 MeV (FWHM) and a source lenght of ~ 20 cm (FWHM).

2. - EXPERIMENTAL APPARATA.

Three of the four interaction regions of Adone are equipped with experimental set-ups; in the fourth a small angle (3^o-6^o) Bhabha scattering detector, which serves as a high rate luminosity monitor, is installed. The luminosity used by the experiments is directly measured by counting wide angle electron pairs detected in each apparatus.

The three set-ups are somewhat complementary since MEA has magnetic analysis, $\gamma\gamma 2$ is oriented toward γ detection and BB uses calorimetric information from large liquid scintillators. They are described in detail in refs. (2, 3, 4) respectively; here I will only summarize their main features.

The $\gamma\gamma 2$ set-up (see Fig. 1) consists of two large semicylindrical telescopes placed above and below the interaction region. These telescopes (shower detector) are a sandwich of scintillation counters, optical spark chambers and lead converters (total thickness 5.5 R.L.). The shower detector covers a solid angle, for a point-like source, of $0.41 \times 4\pi$ sr for triggering and $0.66 \times 4\pi$ sr for detecting tracks and photons.

Outside the shower detector heavy plate optical spark chambers are used to observe the ranges and nuclear interactions of hadrons. A pair of circular side-telescopes containing spark chambers with magnetostrictive read-out, lead absorbers and scintillation counters, complete the detection system ($0.15 \times 4\pi$ sr). The trigger logic requires a coincidence between the upper and lower telescopes of the shower detector. For only a charged par

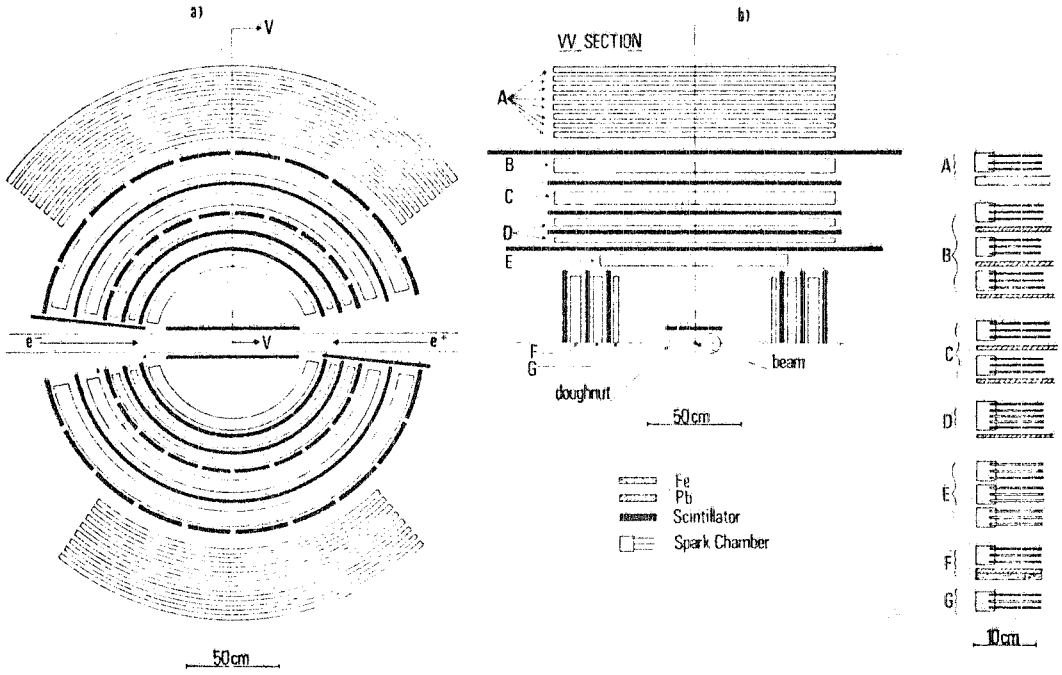

FIG. 1 - $\gamma\gamma 2$ experimental set-up. a) Front view from the center of Adone; b) vertical section in the plane normal to the beams (For the sake of clearness, the side telescopes are not shown in the front view of the apparatus).

ticle in a telescope this corresponds to a lower energy limit of $T_\pi \simeq 120$ MeV, $T_k \simeq 190$ MeV. If photons enter the telescope firing the trigger counters these limits could be as low as $T_\pi \simeq 35$ MeV, $T_k \simeq 60$ MeV.

In February 1978 the $\gamma\gamma 2$ apparatus was modified. A resistive tubes core[8], around the interaction region, was added increasing the total solid angle to $\Delta\Omega = 0.9 \times 4\pi$ (for tracking) and lowering the minimum energy to $T_\pi \simeq 20$ MeV (see Fig. 2). The data collected with this apparatus are well in agreement with the previous data so they are

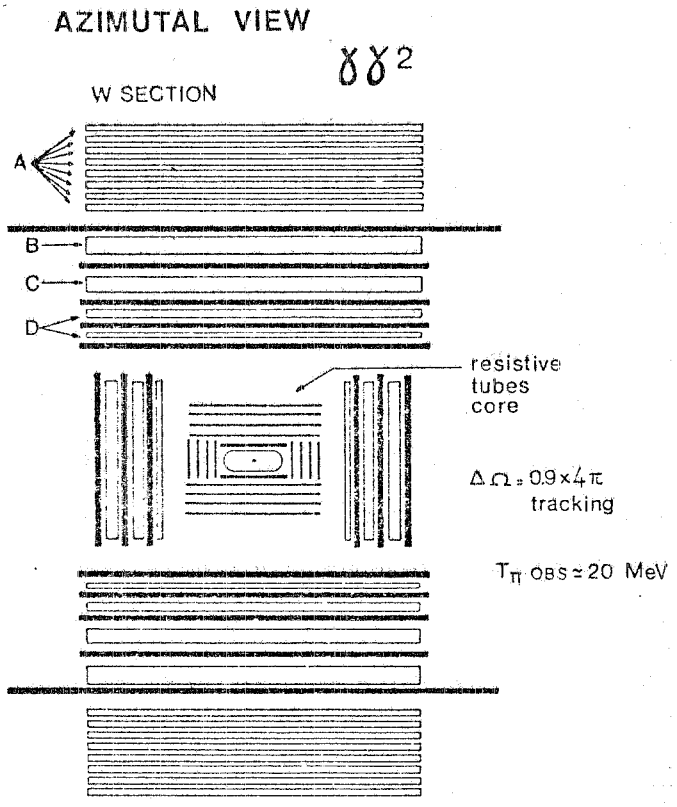

FIG. 2 - Vertical section of the modified $\gamma\gamma$ apparatus.

everywhere averaged.

The MEA detector (see Fig. 3) uses a solenoid, with a 2 meter diameter lenght placed trasversely to the beams. Two compensating magnets are located inside the main coil. The magnetic fields used at these energies were 2 and 2.5 KGauss. Track curvature is measured by the thin optical chambers C_1, C_1' and by the wide gap cylindrical optical spark chambers C_2, C_2'. The solid angle for magnetic analysis is $0.35 \times 4\pi$ sr for point-like source. The momentum resolution is $\Delta p/p = \pm 8\%$ at $p = 0.8$-1 GeV. Outside the coil heavy plate optical spark chambers are placed to identify electromagnetic showers and to observe nuclear interactions and ranges of pions and kaons. The trigger requires two charged particles, respectively in the upper and lower part of the apparatus, to penetrate out to S_4 and S_4' ($T_\pi \simeq 130$ MeV, $T_k \simeq 190$ MeV). From spring 1977 a time-of-flight systems allows a π/k discrimination for $400 \lesssim p \lesssim 600$ MeV/c.

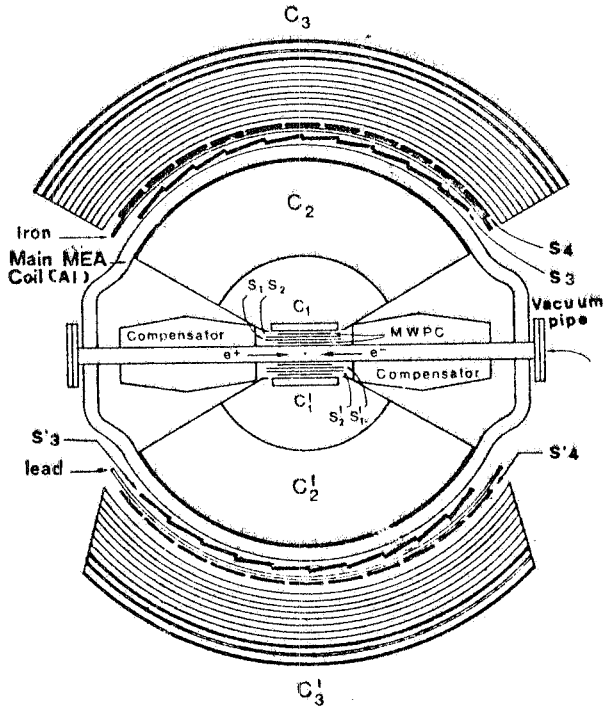

FIG. 3 - MEA experimental set-up (vertical section). C_1, C_1' are narrow gap spark chambers; C_2, C_2' are wide gap cylindrical spark chambers for momentum analysis; C_3, C_3' are thick plate spark chambers for particle identification. MWPC are multiwire proportional chambers; $S_1, S_1', \ldots, S_4, S_4'$ are scintillation counters.

The $\bar{B}\bar{B}$ set-up (see Fig. 4), originally intended to detect $p\bar{p}$ pairs, has cylindrical symmetry with respect to the beam axis. The solid angle covered is $0.7 \times 4\pi$ sr. It is mainly composed of 4 concentric hodoscopes of scintillation counters. Each hodoscope has 16 elements: plastic scintillator tanks (31 gr/cm^2; 0.8 R. L. thick) for HOD3. Two cylindrical magnetostrictive spark chambers sourronding the interaction region are used to measure the direction of the charged particles

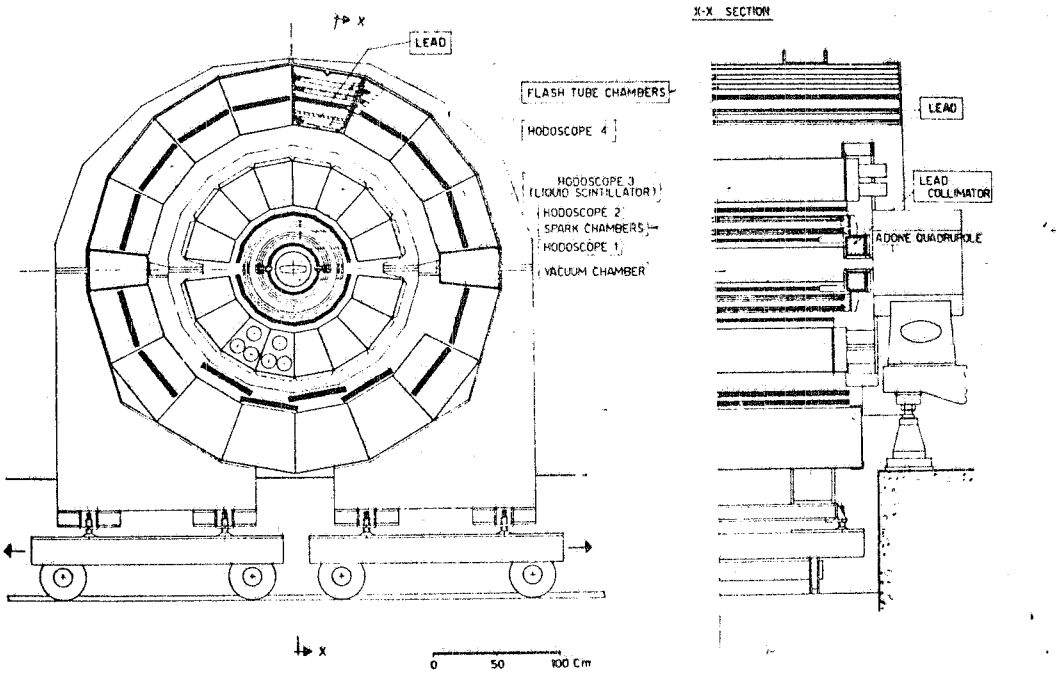

FIG. 4 - $B\bar{B}$ experimental set-up.

To identify electrons and photons the detector is completed by a system of four layers of flash tubes (parallel to the beams) with a lead converter (2.5 R.L.). A track is defined by a coincidence of HOD 1, 2 and 3 in a sector. For pions this corresponds to a minimum energy $T \simeq 60$ MeV. The trigger can require two or three tracks in different sectors. To reduce the background, in the off-line analysis at least one of HOD 4 counters is requested ($T_\pi \gtrsim 200$ MeV).

3. - NEW LIMITS ON $e^* \rightarrow e\gamma$.

A new measurement of $e^+e^- \rightarrow e^+e^-\gamma$ has been performed using set up $\gamma\gamma 2$ together with tagging counters for detecting small-angle electrons.

The results are in agreement with QED predictions as it is shown in the mass spectra of Fig. 5.

Considering the existence of a heavy electron e^* a new upper limit on the coupling constant λ^2 versus $M(e^*)$ is achieved (see Fig. 6), starting from the standard hamiltonian

$$Hi = \frac{e\lambda}{M(e^*)} \quad \psi_{e^*} \sigma_{\mu\nu} \psi_e F^{\mu\nu} + h.e.$$

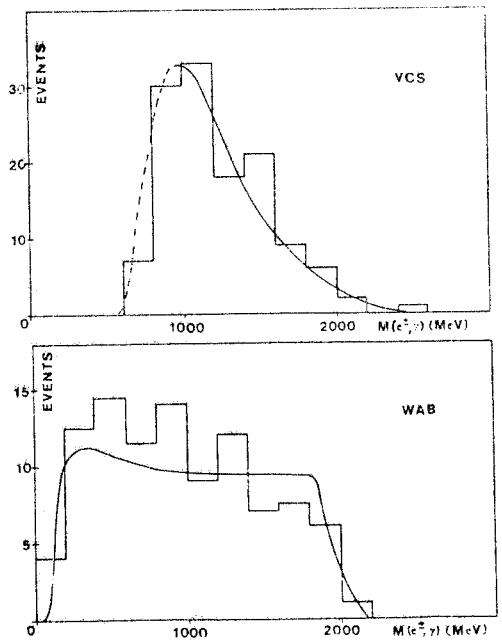

FIG. 5 - Effective mass distribution of the wide-angle ($e^{\pm}$) systems: a) for CS events, with the $e^{\mp}$ in the tagging counters; b) for WAB events, with all the e^{+}, e^{-}, in the wide-angle apparatus. The solid lines are absolute QED predictions.

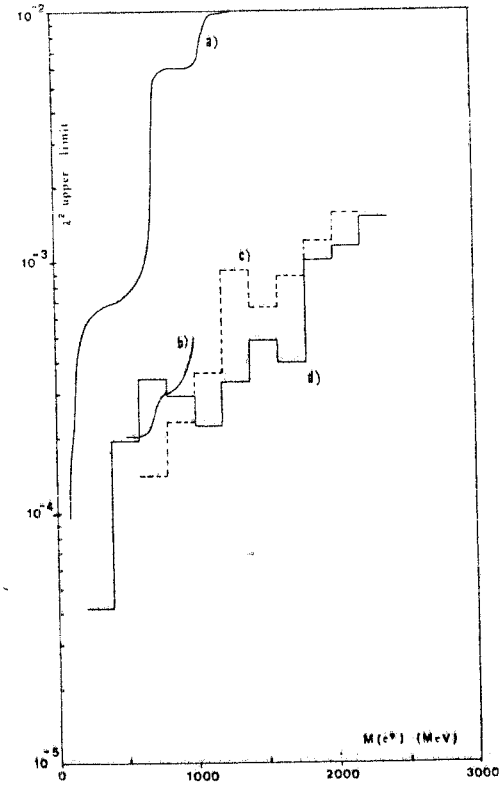

FIG. 6 - Upper limit (95% confidence level) on ^{2} versus the e^* mass: a) Ref. (5); b) Ref. (6); c) Due to a trivial error, the results reported in Fig. 4 of Ref. (7) are not correct. Here we report the corrected values; d) Present results.

4. - R VALUES.

In order to calculate R, multiplicities and partial cross sections, using the standard likelihood method, the following assumptions were made:

a) All particles in the final states are π;

b) Invariant phase space (IPS) momenta distributions;

c) Isospin relation $\langle n^{\pm} \rangle = 2 \langle n^{o} \rangle$ for $n^{\pm} + n^{o} = 5$;

d) Maximum multiplicity $n^{\pm} + n^{o} = 6$ up to 2 GeV and $n^{\pm} + n^{o} = 8$ up to 3.1 GeV.

The first hypothesis is reasonable especially at lower energies. In a more quantitative way the MEA group has measured the percentage of kaons respect to the total prongs in a given momentum window (see Fig. 7). This K fraction is lower than 20%.

Using a special category of events the $\gamma\gamma$ group has also estimated

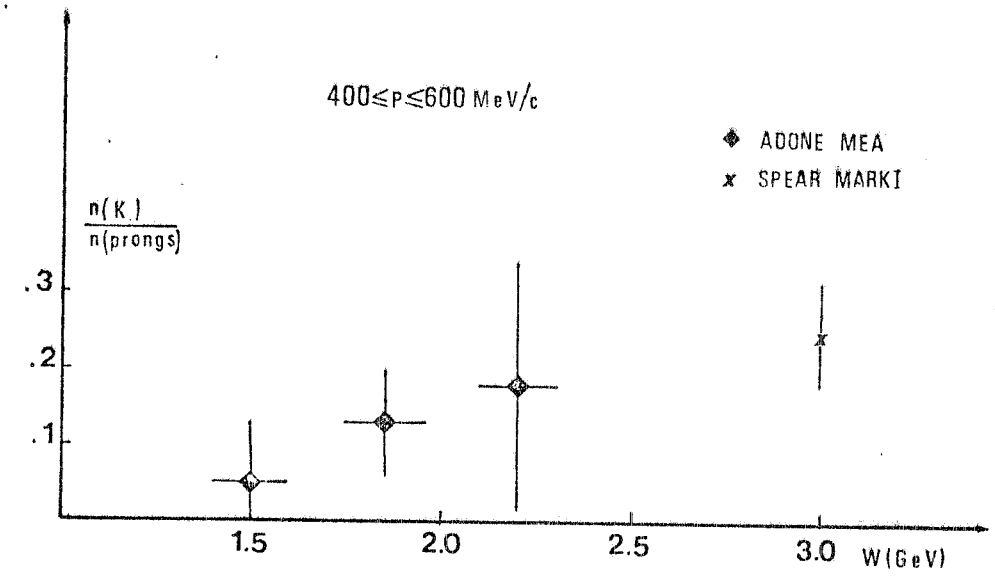

FIG. 7 - Ratio between the numbers of K and prongs whose momentum falls in the range $400 \leq p \leq 600$ MeV/c.

an upper limit at 1.5 GeV for KK^* production of 8 nb (95% c.l.), that is $\sim$ 10% of the total cross section.

The second hypothesis is supported by the invariant distribution reported in Fig. 8 well fitted by a thermodynamical spectrum with KT = 145 ± ± 3 MeV. This result in fact can be independently obtained summing the I.P.S. momentum distributions for each channel weighted with the partial cross sections we will see after.

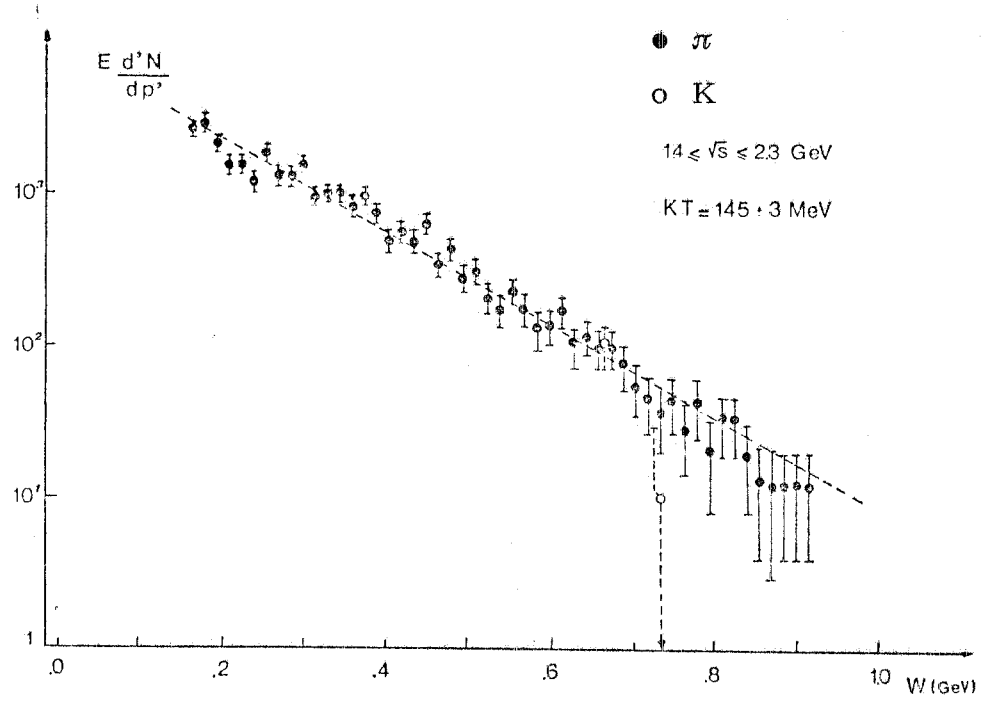

FIG. 8 - Invariant distribution for π and K as function of the total energy of the particle.

The values of R for at least 3π in the final states are reported in Fig. 9 together with a large panorama of already published values[9-14]. The values of VEPP2M are calculated summing the two most important cross sections that are $\sigma(2\pi^+, 2\pi^0)$ and $\sigma(4\pi^+)$.

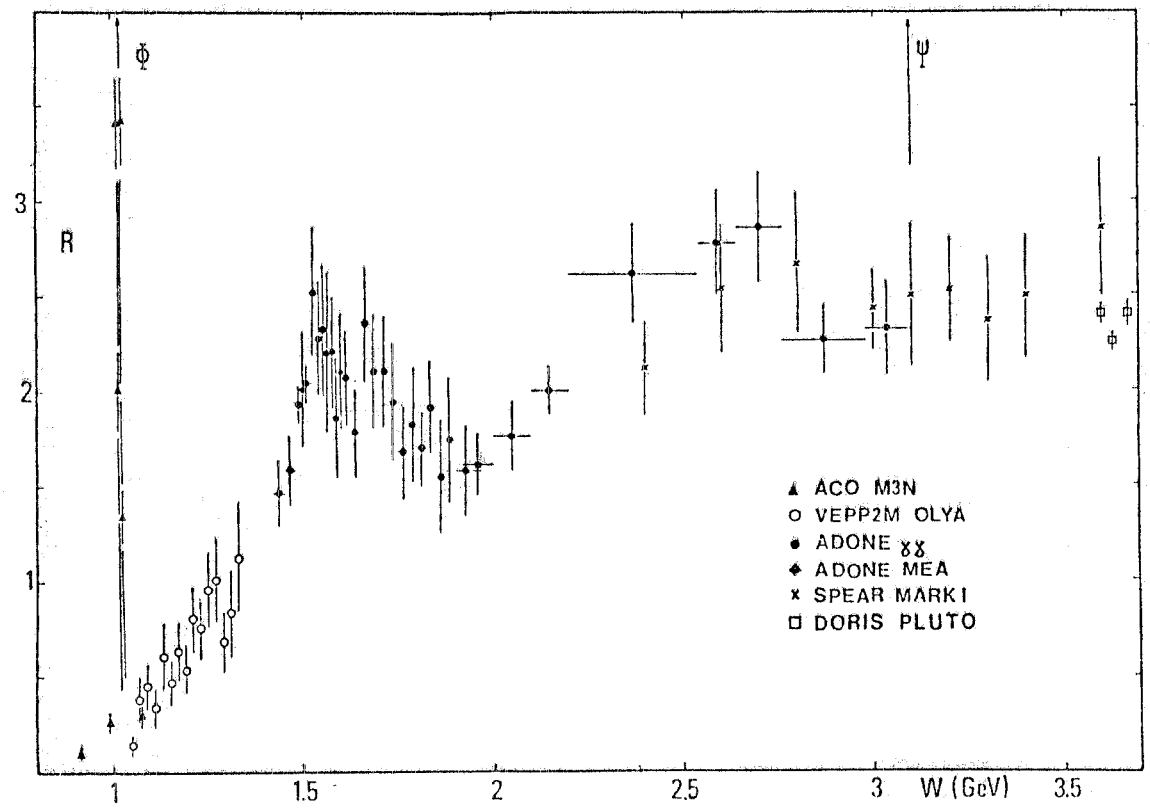

FIG. 9 - R versus total energy.

The quoted errors are statistical only while the systematical ones on $\gamma\gamma$ data are $\sim 20\%$ (due to luminosity, efficiencies, K presence).

The energy behaviour of the ratio R is now rather well established above 1 GeV.

In the low energy region after the ϕ, there is a sharp rise whose pattern is similar to the charm threshold. In this behaviour the more important contribution comes from $\sigma(4\pi^+)$ as we will see later.

More definite predictions come from local duality and EVDM. They essentially predict, around the asymptotic value, a series of oscillations due to the vector meson recurrences. Using the mass formula $\Delta m_i^2 \simeq 1$ GeV^2 and scaling Γ_{ee} and Γ_{tot} with the masses the expected values of R do not fit the data concluding that, as we will see also later, some of these recurrences do not exist or have Γ_{ee} much smaller. On the contrary the asymptotic value of R, calculated by formula $R = 16\pi^2 / \Delta m_\varrho^2 f_\varrho^2 \simeq$

$\simeq 2.5$[15] fits very well the value of R above 2.4 GeV.

Also QCD and asymptotic freedom predict a value R = 2.3 between 2.4 GeV and 3.6 GeV, that rather well fits the data.

5. - MULTIPLICITIES, G-PARITIES.

Mean charged multiplicity is reported in Fig. 10. As a reference the extrapolation of a logarithmic fit to the high energy data[13] is reported.

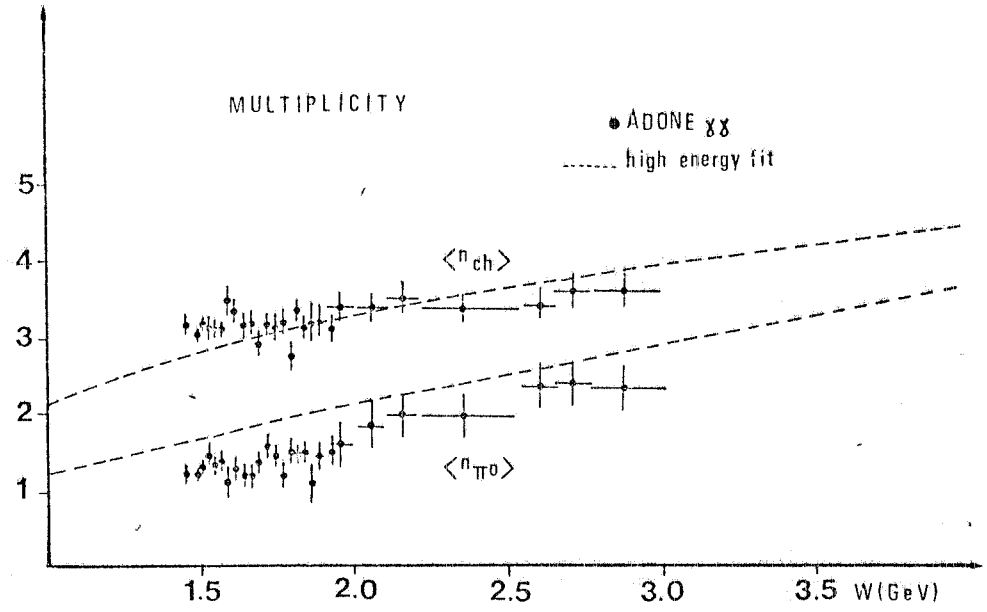

FIG. 10

In the same figure the mean $\langle \pi^o \rangle$ multiplicity is also reported, together with the extrapolation on what is expected from the missing energy in the same high energy data[13], assuming $\langle E_{\pi^\pm} \rangle = \langle E_{\pi^o} \rangle$.

In Fig. 11 the ratio between the mean charged and π^o multiplicities is considered: this ratio must to be compared with the value 2, which is expected on statistical ground if only pions would be present.

At high energies an excess of neutral energy is present, usually interpreted as η production, whose threshold is around 2 GeV. At low energies an excess of charged particles emerges. This is expected by the isovector resonance $\varrho''(1.6)$ dominance (a process like $\varrho''(1.6) \to \varrho\pi\pi$ (S-wave) contributes with a ratio 5).

Before considering the various reactions which contribute to the total cross section, let us divide them in two categories, according to the G parities. The total cross section for even, G^+, and odd, G^-, number

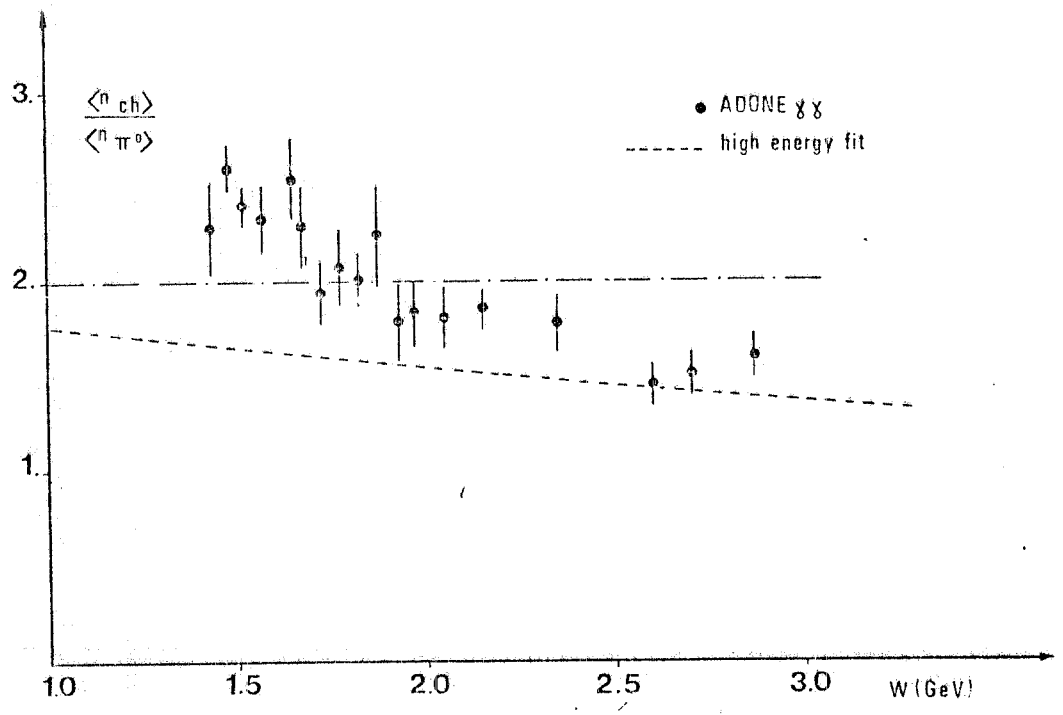

FIG. 11

of pions are reported in Fig. 12 ($n \geq 3\pi$) and the ratio G^-/G^+ is reported in Fig. 13.

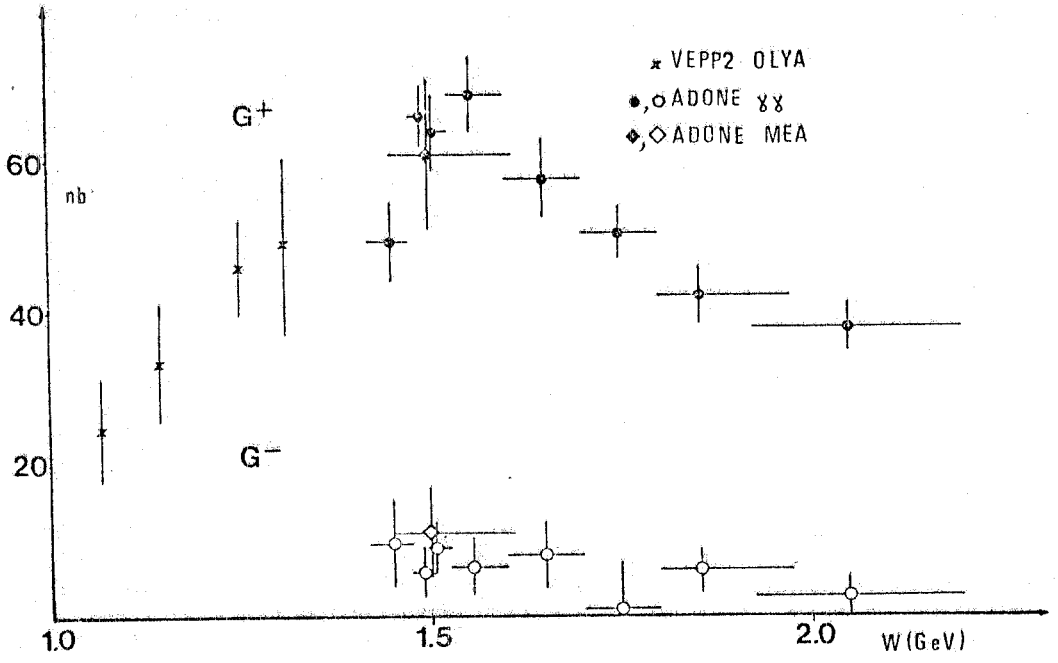

FIG. 12 - G^+ (sum of $\sigma(n\pi)$ with n even) and G^- (sum of $\sigma(n\pi)$ with n odd) versus total energy.

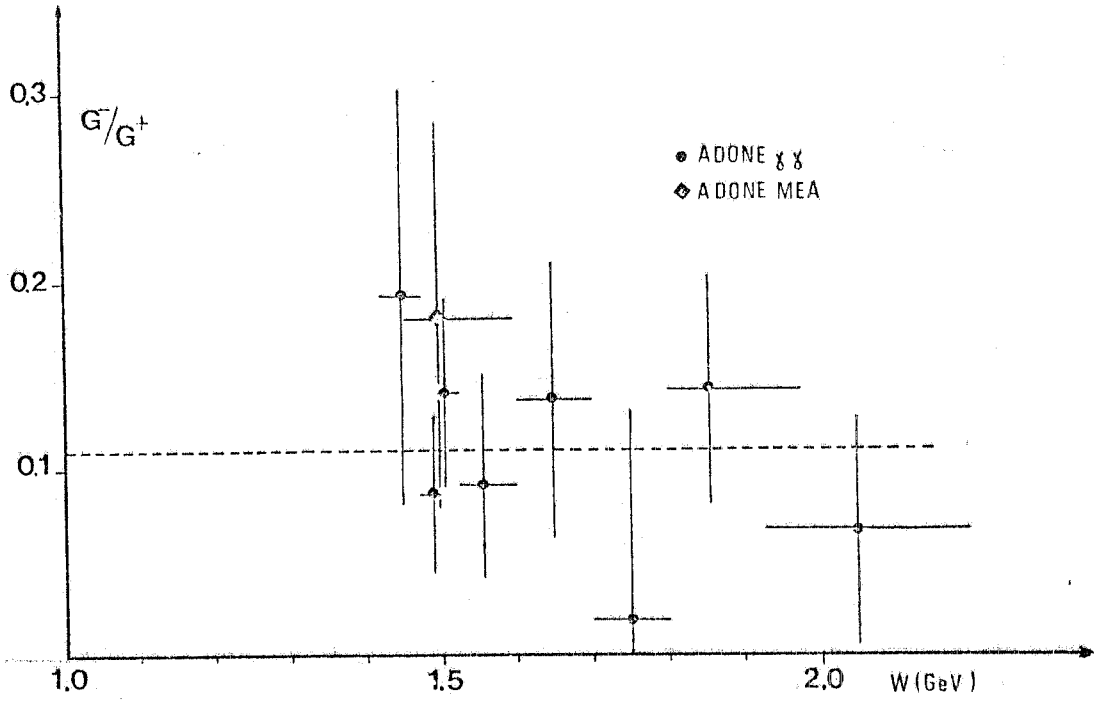

FIG. 13

SU_3 predicts :

$$\frac{|A(e^+e^- \to \omega\text{-like} \to G^-)|^2}{|A(e^+e^- \to \varrho\text{-like} \to G^+)|^2} = \frac{|Q_u + Q_d|^2}{|Q_u - Q_d|^2} = \frac{1}{9} = \frac{\Gamma_e(\omega\text{-like})}{\Gamma_e(\varrho\text{-like})}$$

which is a prediction on the ratio of the integrated cross sections.

Basing on these considerations we can deduce that also the ratio G^-/G^+ between the cross sections as function of energy is expected to lie around the value 1/9, as the measured values roughly show.

6. - PARTIAL CROSS SECTIONS.

6.1. - $\sigma(\pi^+\pi^-\pi^+\pi^-)$.

The better established channel is the 4 charged pions. The $\gamma\gamma$ and MEA values are reported in Fig. 14 together with those already published[9-13, 17]. The general behaviour looks like as a resonant one. The dotted line represents a best fit over all the values with only one relativistic Breit-Wigner with an energy dependent width for threshold effect (for sake of simplicity assumed as for the ϱ) according to the following formulas :

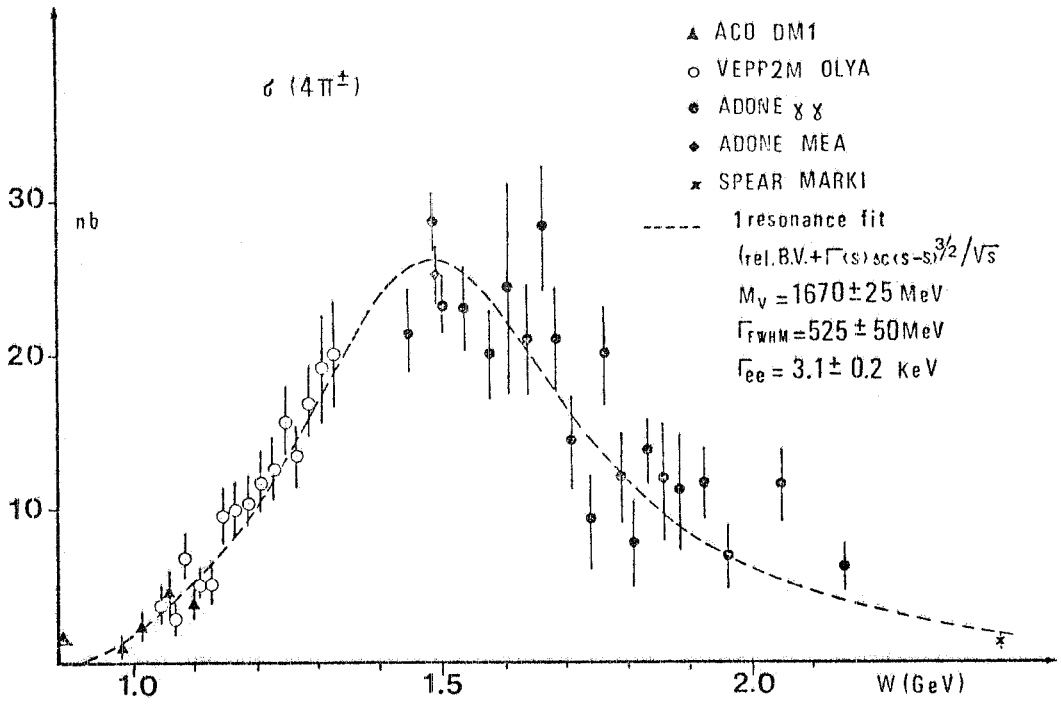

FIG. 14

$$= \frac{12\pi}{s} \frac{M_V^2 \Gamma_V \Gamma_{ee}}{(s - M_V^2)^2 + M_V^2 \Gamma_V^2} \quad , \qquad \Gamma_V = K \frac{(s - M_o^2)^{3/2}}{\sqrt{s}} \quad .$$

The result of the fit gives the following parameters :

$$M_V = 1670 \pm 25 \text{ MeV} \quad , \quad \Gamma_{FWHM} = 525 \pm 50 \text{ MeV} \quad , \quad \Gamma_{ee} = 3.1 \pm 0.2 \text{ keV}.$$

All these parameters are in a rather good agreement with those known of the $\varrho''(1.6)$.

Dynamical correlations in the final state are studied by the MEA group. In Fig. 15 the invariant mass spectrum of the 2 prongs neutral system are reported for all the events. Only at the ϱ mass a significant peak is present.

Selecting the 4 prongs events the corresponding Dalitz plot is shown in Fig. 16. The result largerly favours a $\varrho\pi\pi$ intermediate state.

6.2. - $\sigma(\pi^+\pi^-\pi^o\pi^o)$.

The second large cross section is that with 2 charged plus 2 neutral pions in the final state. The $\gamma\gamma$ and MEA values are reported in Fig. 17 together with those already published. This cross section shows a rather different behaviour respect to the $\sigma(4\pi^{\pm})$.

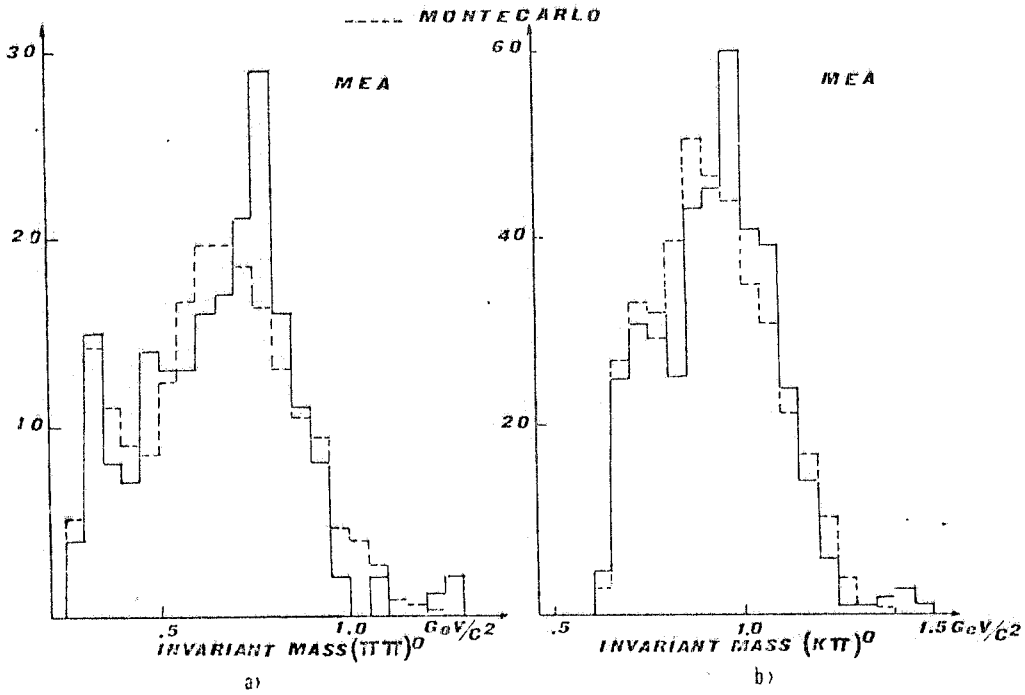

FIG. 15 - Invariant mass distribution for 2 prong neutral system. Each track is assumed to be a π (a), or alternatively a K or a π (b).

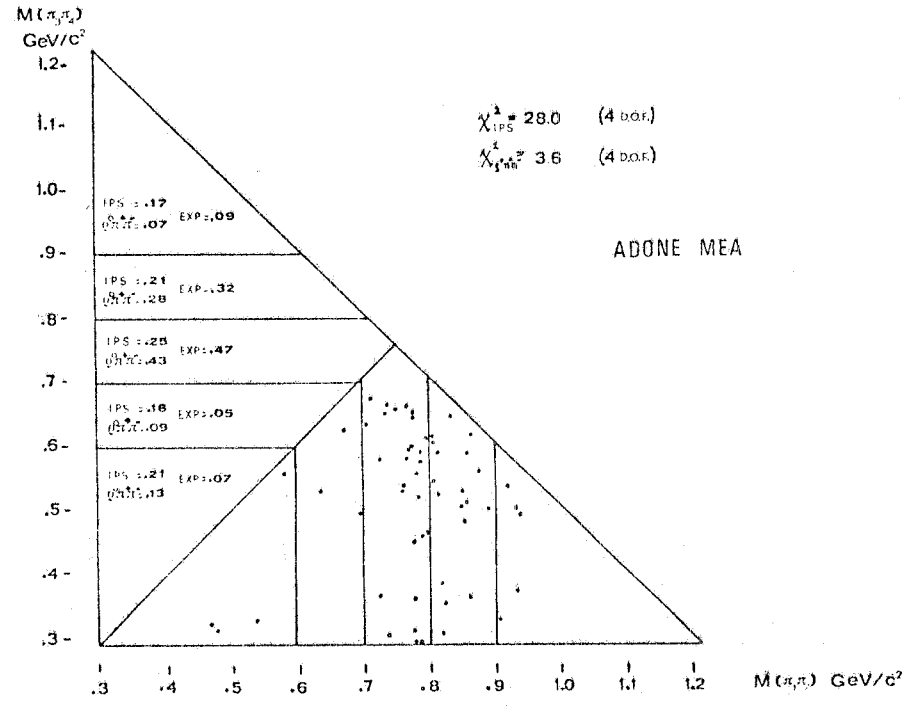

FIG. 16 - Scatter plot of the invariant mass of oppositely charged pion pairs, $M(\pi_1\pi_2)$ vs the invariant mass of the remaining pair $M(\pi_3\pi_4)$.

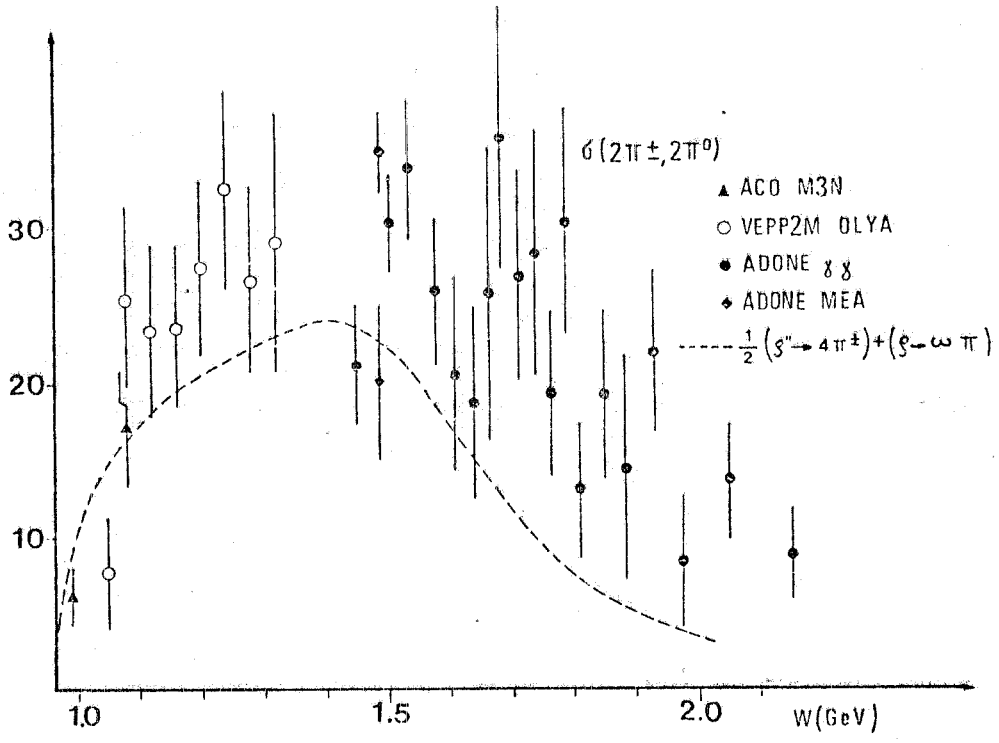

FIG. 17

Two contributions must be taken into account. First, the ϱ-tail going into $\omega\pi$, computed by Renard[16] starting from the $\omega \to \varrho\pi$ decay. Second, the $\varrho''(1.6)$ decay via $\varrho^{o}\pi^{o}\pi^{o}$ whose cross section can be taken as $\frac{1}{2}\,\sigma(4\pi^{\pm})$, if the two $\pi\pi$ are in S-wave. A simple sum of these two contributions is reported (dotted line) also in Fig. 17. The measured values are everywhere over this curve so other contributions must be present.

In the low energy region only a small room (5-10 nb) is possible. On the contrary around 1.25 GeV the first ϱ-recurrence is expected. Local duality, that works rather well on J/ψ and Υ families, gives[18]:

$$\left(\frac{m\,\Gamma_{ee}}{\Delta m^2}\right)_{\varrho} = \left(\frac{m\,\Gamma_{ee}}{\Delta m^2}\right)_{\varrho'} = \left(\frac{m\,\Gamma_{ee}}{\Delta m^2}\right)_{\varrho''} .$$

Applying this formula to the $\varrho''(1.6)$, we obtain, within a factor 2, the values quoted above.

For the $\varrho'(1.25)$ we obtain, using $\Delta m^2 \simeq 1\ \mathrm{GeV}^2$ and $\Gamma \simeq 200\ \mathrm{MeV}$, a peak cross section of about ~ 200 nb, wich is an order of magnitude bigger than the available cross section.

6.3. - $\sigma(4\pi^{\pm}, 1\pi^{o})$ and $\sigma(4\pi^{\pm}, 2\pi^{o})$.

The separation between these two channels is a very critical one: it depends essentially on how well the photon detection efficiency is known. For the $\gamma\gamma$ apparatus this efficiency has been cecked on the observed photons taking so in account also the optical spark chamber efficiency for multisparks. However the sum of these two cross sections has not been affected by the photon efficiency and is reported in Fig. 18. The value centered at 1.82 GeV shows the effect of the already published resonance[19].

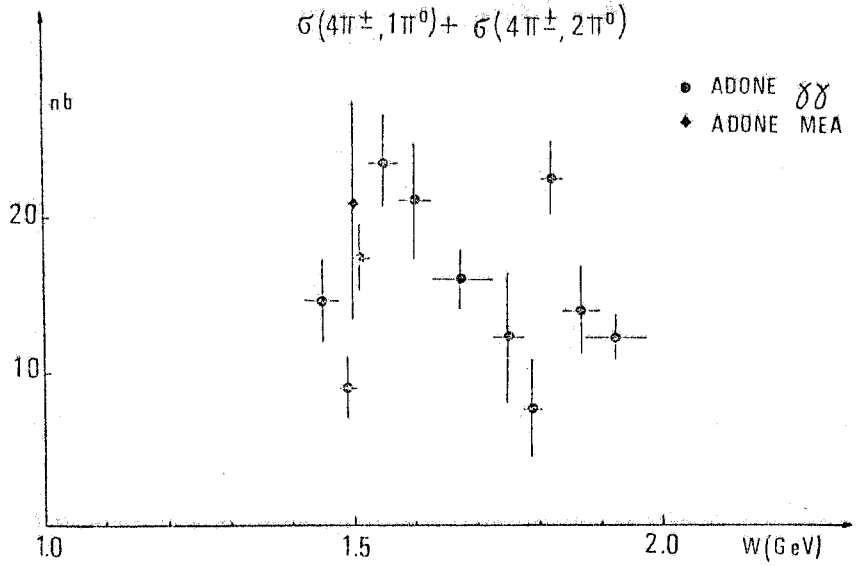

FIG. 18

In Fig. 19 the $\sigma(4\pi^{\pm}, 1\pi^{o})$ is reported. Over all the range explored this cross section is rather small. This smallness is in agreement with the SU_3 prediction for the ratio G^{-}/G^{+} because the $\sigma(4\pi^{\pm}, 1\pi^{o})$ gives the bigger contribution to the quantity G^{-}.

The $\sigma(4\pi^{\pm}, 2\pi^{o})$, reported in Fig. 20, shows everywhere values rather high.

6.4. - $\sigma(\pi^{+}\pi^{+}\pi^{o})$.

At last in Fig. 21 the $\sigma(\pi^{+}\pi^{-}\pi^{o})$ is reported. This cross section has values rather near to zero.

At 1.66 GeV, the energy of the resonance found at DCI in this channel, we have also, in spite of the poor statistics collected in this region, a poor indication of this resonance using two different category of events.

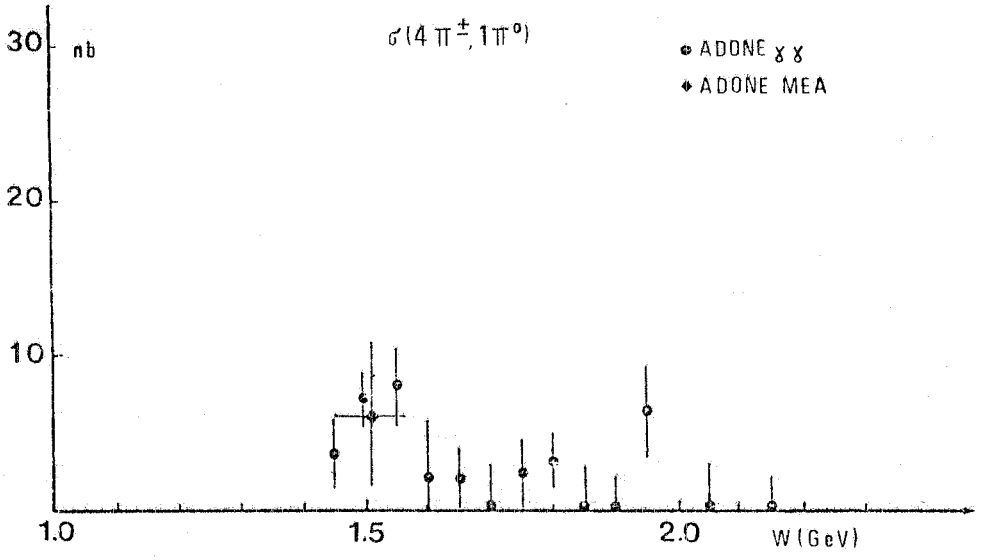

FIG. 19

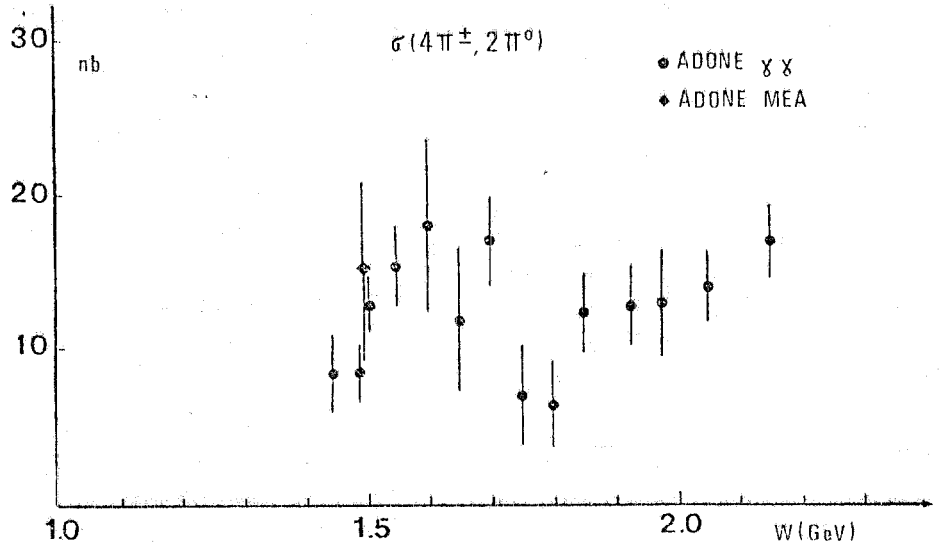

FIG. 20

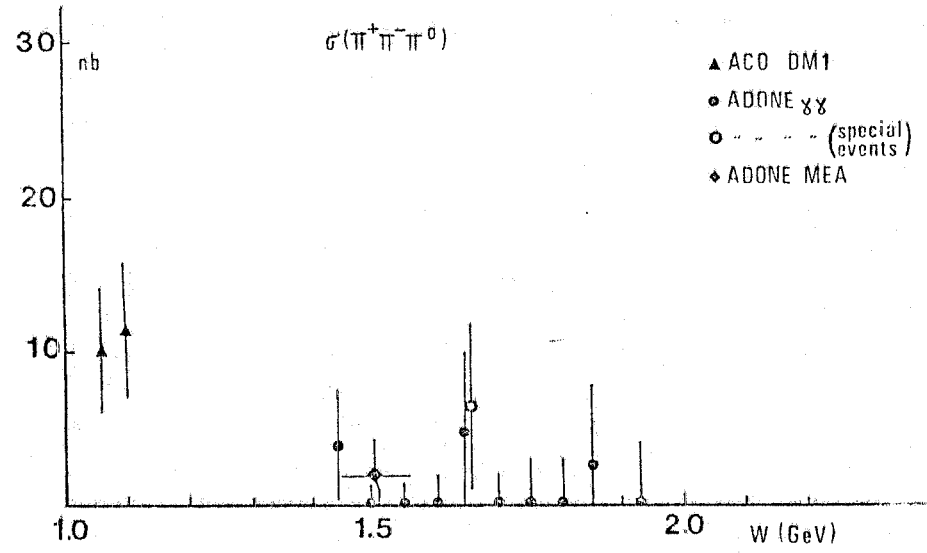

FIG. 21

In conclusion the panorama of e^+e^- annihilation under 3 GeV starts to become clearer but, nevertheless, a lot of problems are still open. First of all we want remember the real existence of all the members of the vector mesons families.

REFERENCES AND FOOTNOTES.

1) List of authors :

FRASCATI-NAPLES-PISA-ROME	FRASCATI-ROME BOLOGNA	FRASCATI-MARYLAND-NAPLES-PADUA-ROME
$B\bar{B}$	$\gamma\gamma 2$	MEA
M. Ambrosio	C. Bacci	R. Bernabei
G. Barbarino	R. Baldini-Celio	S. D'Angelo
G. Barbiellini	R. Battistoni	B. Esposito
A. Barletta	G. Capon	F. Felicetti
C. Bemporad	R. Del Fabbro	A. Marini
R. Biancastelli	G. De Zorzi	P. Monacelli
G. Brosco	E. Iarocci	A. Nigro
M. Calvetti	M. Massai	M. Nigro
M. Castellano	S. Morigi	L. Paoluzi
F. Costantini	G. P. Murtas	P. Patteri
G. Giannini	G. Penso	L. Pescara
P. Lariccia	M. Spinetti	G. Piano Mortari
G. Paternoster	L. Trasatti	P. Rosini
S. Patricelli	B. Stella	F. Ronga
L. Tortora	D. Ballim'	A. Sciubba
U. Troya		A. Sebastiani
		B. Sechi-Zorn
		F. Vanoli

2) C. Bacci et al., Phys. Letters 64B, 356 (1976).
3) W. W. Ash et al., Frascati report LNF-77/18 (1977); Lett. Nuovo Cimento 11, 705 (1974).
4) G. Barbiellini et al., Phys. Letters 68B, 397 (1977).
5) C. D. Baley et al., Phys. Rev. 167, 1275 (1967).
6) H. J. Beherend et al., Phys. Rev. Letters 15, 900 (1965).
7) C. Bacci et al., Phys. Letters 44B, 530 (1973).
8) G. Battistoni et al., Nuclear Instr. and Meth. 152, 423 (1978).
9) V. A. Sidorov, Comm. to High Energy Physics Conf., Tblisi (1976).
10) G. Parrour et al., Phys. Letters 63B, 357, 362 (1976).
11) B. Esposito et al., Lett. Nuovo Cimento 19, 21 (1977).
12) R. Baldini et al., Lett. Nuovo Cimento 24, 324 (1979).
13) J. E. Augustin et al., Phys. Rev. Letters 34, 764 (1975); R. F. Schwitters, Proc. of 1975 Intern. Symp. on Lepton and Photon Interaction, Stanford (1975).
14) G. Knies, Comm. to Lepton-Photon Interaction Symp., Hamburg (1977).

15) M. Greco, Nuclear Phys. 63B, 398 (1973).
16) F. M. Renard, Nuovo Cimento 64A, 979 (1969).
17) A. Cordier et al., Orsay report LAL 78/31 (1978).
18) M. Greco, Phys. Letters 77B, 84 (1978).
19) B. Esposito et al., Phys. Letters 68B, 389 (1978); C. Bacci et al., Phys. Letters 68B, 393 (1978); G. Barbiellini et al., Phys. Letters 68B, 397 (1978).